SNO-STR-95-054

DRAFT DRAFT DRAFT DRAFT DRAFT DRAFT

^{8}Li: A β Calibration Source for SNO

B. Sur, E. D. Earle, R. Deal and E. Gaudette,
A.E.C.L., Chalk River Laboratories, Chalk River Ontario K0J 1J0

ABSTRACT

We propose to use β^- particles from the decay of ^{8}Li to calibrate the response of the Sudbury Neutrino Observatory [SNO] detector to high energy electrons. The ^{8}Li will be produced by the ^{11}B(n,α) reaction with 14-MeV neutrons from a small deuterium tritium [DT] neutron generator, located about 50 m away from the SNO detector cavity. The short-lived ($t_{1/2}$=0.838 s) ^{8}Li recoil atoms from the solid ^{11}B target foils will be transported by aerosol particles in a helium gas stream flowing through a flexible capillary tube. The transported activity will decay inside a wire chamber inside the D_2O volume of SNO, so that ^{8}Li decays can be identified by the signal from the 2-α decay of its daughter ^{8}Be* nucleus. We have verified the principles and the yields from this proposed calibration scheme by experiments conducted at the Tandem Accelerator and Super-Conducting Cyclotron (TASCC) facility and the D-T neutron generator facility at Chalk River Laboratories (CRL).

1. INTRODUCTION

The SNO detector will determine the energy spectrum of solar neutrinos by detecting electrons produced in the Charged Current [CC] detection reaction:

$$\nu_e + d \rightarrow p^+ + p^+ + e^- \qquad Q = -1.44 \text{ MeV} \qquad (1)$$

The electrons will be detected by means of the Cerenkov radiation they produce in the heavy water which constitutes the neutrino detection medium in the detector. The energy resolution of the detection scheme is expected to be about 10%, and the threshold above which the solar neutrino spectrum will stand out from low-energy background events is expected to be approximately 5 MeV. Thus, SNO will be sensitive mainly to solar neutrinos with an end-point energy of 14 MeV from the decay of ^{8}B to the broad first excited state in ^{8}Be.

The neutrino spectral shape as measured in the SNO detector will be a crucial tool in deciphering the solar neutrino problem. In conjunction with the flavor independent non-sterile neutrino flux determined by the neutral current [NC] signal, it will allow the unambiguous determination of mass and mixing parameters in either MSW or sterile neutrino oscillation scenarios if they exist. The undistorted CC spectral shape is expected to be that of ^{8}B ν's folded with the CC energy dependent cross-section and corrected for the ~ 2% energy shift due to the recoiling protons, and the 1.44 MeV shift due to the CC threshold. The cross section and kinematic effects can be calculated to ~ 5% accuracy due to the simple nuclear structure of the deuteron. The undistorted ^{8}B ν spectral shape can then be virtually recreated by observing the β^- decay of ^{8}Li.

The decay of ^{8}Li is the mirror decay of ^{8}B. It β^- decays to the same broad first excited state in ^{8}Be with a β^- end-point energy of 13 MeV and a half-life of 0.84 s [Ref. 1]. Moreover, the ^{8}Li β^- decay is followed immediately by the break-up of the daughter ^{8}Be* nucleus to two α-particles with kinetic energy of 1.7 MeV energy each. The detection of these α-particles can thus be used as a tag or trigger to ensure that only ^{8}Li decays are studied as opposed to background events.

We propose to produce ^{8}Li for calibrating the SNO detector by the ^{11}B(n,α) reaction, using 14-MeV neutrons from a DT generator and a solid ^{11}B target foil. ^{8}Li recoils from the surface layers of the target foil will be thermalized, and captured by aerosol particles in a He gas stream. Laminar flow of the He gas in a teflon capillary tube will be utilized to rapidly transport the aerosol particles carrying the activity to a thin-walled wire chamber located inside the SNO D_2O volume. The wire chamber, also called the ^{8}Li decay chamber, will be used to tag ^{8}Li decays by detecting the ^{8}Be* α-decay signal. We report here on an experimental test of this scheme at the CRL DT generator facility. The purpose of these tests was to (a) measure the yield of ^{8}Li recoil atoms per 14-MeV neutron, (b) verify the efficiency of the He gas - aerosol transport scheme, and (c)

study the rate and suppression schemes for contaminant products. The primary contaminant is expected to be 13.8 s ^{11}Be made by the ^{11}B(n,p) reaction.

2. CALCULATION OF YIELDS AND EFFICIENCIES.

2.1 Recoil Yield from the Target.

The Q-values, cross-sections (at 14-MeV neutron energy), maximum recoil energy, and the corresponding maximum ranges in two candidate target foil materials, for the heavy product nuclei are shown in Table 1.

Table 1: Characteristics for reactions in the proposed scheme.

Reaction	Q (MeV)	σ^* (mb)	Max. E_{recoil} (MeV)	Max. Range (mg cm^{-2}) in BN	Max. Range (mg cm^{-2}) in $(CH_2)_n$-B
^{11}B(n,α)^{8}Li	-6.63	30.5	5.4	2.27	2.26
^{11}B(n,p)^{11}Be	-10.72	5 - 25	1.8	0.6	0.56

* Ref. 2

There is a discrepency in the literature for the value of the (n,p) cross-section. The candidate target materials are boron nitride (BN) and 97% isotopically enriched ^{11}B powder held by a 10% polyethylene matrix. Since only recoils are collected, the maximum range corresponds to the effective target thickness for each reaction. These ranges have been calculated using the code TRIM. There are large uncertainities associated with these calculated ranges because of energy straggling, large angle scattering and lack of experimental range data at these very low ion energies. Ignoring such effects, it is possible to write the following analytical expression for the yield, Y_n , of recoil product atoms in the "forward" direction per normally incident neutron:

$$Y_n = \frac{\sigma}{2} \int_{Cos\theta=1}^{Cos\theta=0} \frac{d\Omega_{CM}(\theta_{lab})}{d\Omega_{lab}} \times R[E_{recoil}(\theta_{lab})] \times Cos\theta_{lab} d(Cos\theta_{lab}) \qquad (2)$$

where σ is the total cross-section, assumed to be isotropic in the CM frame, the second term is the forward "boost" to the cross-section due to the kinematics, and R[...] is the range corresponding to the recoil energy E_{recoil}, which itself is determined by the kinematics of the product nucleus emmitted at laboratory angle θ_{lab} with respect to the incident neutron direction.

The above integral can be numerically (Monte-Carlo) evaluated with ranges taken from TRIM. According to this calculation, the fraction of product atoms within the effective target thickness (i.e. maximum recoil range) which actually recoil out of the target is 0.288 and 0.51 for ^{8}Li and ^{11}Be respectively. This gives $Y_n(^{8}Li) = 3.35 \times 10^{-7}$ and $Y_n(^{11}Be) = (0.3 - 1.45) \times 10^{-7}$ for a BN target which has a ^{11}B content of 35% by

weight. In the polyethylene-^{11}B matrix (87% ^{11}B) the calculated yields per neutron are 8.4×10^{-7} for ^{8}Li and $(0.7 - 3.65) \times 10^{-7}$ for ^{11}Be. The yield for a point neutron source behind a disc shaped target, as was used in the actual experiment is found by similar calculations to be consistent with the above numbers. The yield in the backwards direction (w.r.t. the incident neutrons) is calculated to be about 10% of the forward yield. In our experiments, however, the backward yields were not utilized or measured because of the experimental awkwardness and the low incremental gain in yield.

The lower recoil energy and range of the unwanted ^{11}Be can be used to differentially attenuate its recoil yield by covering the target foil with a thin inert or "dead" layer of material. The maximum range of these ^{11}Be nuclei is 0.45 mg cm^{-2} in polypropylene ($[C_2H_4]_n$). Thus a "dead layer" of this thickness covering the ^{11}B target will completely stop the ^{11}Be recoils at the cost of reducing the yield of ^{8}Li recoils to about 40%. We have also attempted to experimentally verify this concept for ^{11}Be suppression.

2.2 Decay Rate in the Decay Chamber.

The production rate of ^{8}Li or ^{11}Be atoms in the target chamber is given by multiplying the yield per neutron, Y_n by the neutron flux integrated over the target area. To obtain the decay rate in the decay chamber, however, requires an evaluation of three transmission factors which correspond to the fraction of product atoms which (i) are delivered out of the target chamber, (ii) survive the transportation to the decay chamber, and (iii) decay in the decay chamber before being swept out by the gas stream. These factors are formulated in this section.

For a target chamber of volume V_{tgt}, with a gas mass flow rate Q, at pressure P_{tgt}, the mean gas residence time or turnover time, τ_{tgt} is given by $(V_{tgt} \times P_{tgt})/Q$. If the reaction products and the carrier gas are assumed to be fully mixed in the chamber, it is easily shown that the fraction of product atoms of mean life τ which are carried out of the target chamber is:

$$\varepsilon_{tgt} = \frac{1}{1 + \frac{\tau_{tgt}}{\tau}} \tag{3}$$

Next, some of the radioactive nuclei are "lost" due to decay during transportation in the capillary tube. The time taken by the gas to traverse this line, t_{trans} is calculated by integrating the time spent along the longitudinal dimension, x, of the tube of cross sectional area, A, and length, l:

$$t_{trans} = \int_0^l \frac{P(x)}{Q} A dx \tag{4}$$

where $P(0) = P_{tgt}$, $P(l) = P_{dec}$ is the pressure in the decay chamber. For laminar flow according to Poiseuille's law:

$$P(x) = \left\{ P_{tgt}^2 - \left(\frac{P_{tgt}^2 - P_{dec}^2}{l} \right) x \right\}^{\frac{1}{2}} \quad (5)$$

The fraction of radioactive atoms that survive this transport time is then:

$$\varepsilon_{trans} = 1 - \exp\left(-\frac{t_{trans}}{\tau} \right) \quad (6)$$

Finally, the fraction of decays that are observed in the decay chamber is given by:

$$\varepsilon_{dec} = \frac{1}{1 + \frac{\tau}{\tau_{dec}}} \quad (7)$$

where the mean residence time of the gas in the decay chamber $\tau_{dec} = V_{dec} \times P_{dec} / Q$.

Thus if the observed decay rate is R_{dec} after correction for detector efficiency, then the production rate in the target chamber is given by:

$$R_{tgt} = R_{dec} \times \varepsilon_{tgt} \times \varepsilon_{trans} \times \varepsilon_{dec} \quad (8)$$

3. EXPERIMENTS AT THE CRL D-T GENERATOR FACILITY

The experimental test of the ^{8}Li calibration system was carried out at the D-T generator facility in the Health Physics Department at Chalk River Labs. The experimental set-up is shown schematically in figure 1. Isotropic 14-MeV neutrons were generated at a water cooled TiT_2 target located at the end of the 150 KeV, 1.5 mA D beam-line. The target chamber was a stainless steel cylinder of length 5.3 cm and ID 3.8 cm. It was placed immediately adjacent to the neutron source, with the disc shaped ^{11}B target foil located on the internal face closest to the source. The aerosol loaded He transport gas was introduced by several 1/4" lines located close to the target end of the chamber. The opposite face of the chamber was a plate with seven short SS capillaries welded into it for the gas outlet. These capillaries were collected together into a single SS block which was then connected via a 1/4" to 1/8" "Cajon" quick-connect fitting to the teflon capillary gas transport tube. The aerosol particles were generated by flowing the incoming He gas through a quartz oven tube containg reagent grade NaCl. Adequate and stable aerosol loading was obtained by maintaining the oven tube temperature between 600 and 630 °C, just below the melting point of NaCl.

The gas supply cylinder, gas flow instrumentation, decay chamber and detectors were located outside the thick concrete neutron shielding walls of the D-T generator vault. Gas inlet lines (1/4" OD polyflow) and capillary transport lines (2.4 mm ID teflon) were connected via an angled cable conduit through this wall. Gas pressures at the target chamber (gas cylinder) and decay chamber (gas exhaust) were measured by Bourdon gauges, while the mass flow rate was measured (and controlled) by an MKS 1159 gas

flow controller. The gas flow meter was previously calibrated for Helium gas by a standard wet test meter.

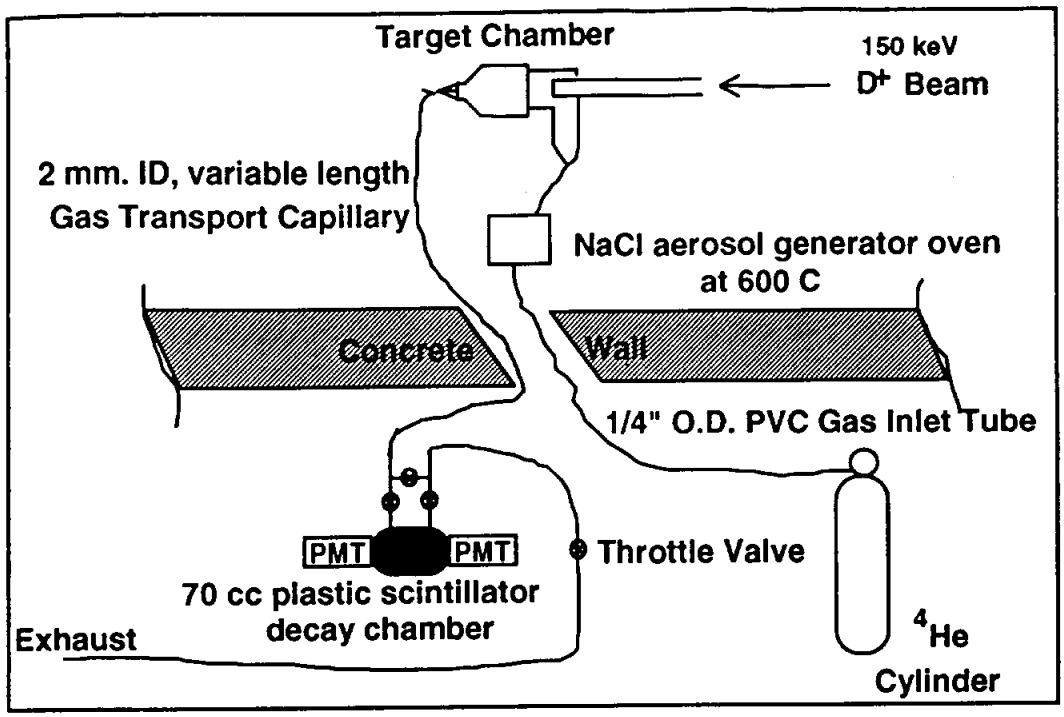

Figure 1: Schematic of the $^{11}B(n,\alpha)^{8}Li$ Experiment.

The capillary transport line was installed in three 50 ft sections. Thus the total length of the line could be chosen to be 50, 100 or 150 ft. To simulate extreme conditions, one of the 50 ft sections was tightly coiled, and one was loosely coiled.

The detection signal for ^{8}Li is β^- particles with 13-MeV end-point energy and a 0.840 s half-life. Initially a decay chamber with a thin Al wall and a 2.5 cm thick plastic scintillator paddle as detector was tried. This configuration yielded a detection efficiciency of $\leq 15\%$ and a noise (i.e. background) rate of 3 s^{-1}. Later experiments were carried out with a decay chamber made out of plastic scintillator material, so that the β^- detection efficiency would be close to 100%. The decay/detection chamber was viewed by two photimultiplier tubes (PMT's) whose signals were individually amplified and gated with a threshold discriminator. The energy signals above the discriminator level, chosen so as to maximise the signal to noise, were then added and counted by a CANBERRA Series 35 Multi Channel Analyser in either pulse height analysis or multi-scaling mode. The relatively thin (1 cm) walls of the scintillator decay chamber however precluded an energy spectrum measurement of the β particles. Also this decay chamber was of fragile construction and the plastic bonds had minute gas leaks. Thus it could not be operated above ambient pressure i.e. 1 atm. To measure the characteristic half-lives of the β activity, the He gas and aerosol carrier had to be confined. To achieve this, a system of

solenoid gate valves, consiting of an inlet and outlet valve and a bypass valve were connected to the decay chamber. For filling the chamber, the bypass valve was closed and the inlet-outlet valves were opened so that the aerosol loaded gas flowed through the chamber. To measure the decay half-life, the inlet and outlet valves were closed, while the PMT signals were counted in time bins (i.e. multi-scaled). The bypass valve was opened during this period to maintain the gas flow conditions, which otherwise would require several tens of seconds to stabilize. The operation of the solenoid valves and the simultaneous start and reset of the MCS cycles were done automatically by TTL signals generated by a Phillips Model 795 Quad Gate and Delay Generator module.

The neutron beam flux was monitored by scaling pulses from a plastic-scintillator counter in a fixed geometry near the D-T neutron source. The flux sensitivity of this counter had previously been determined by cross-calibrating it with an ^{56}Fe foil activation. The experiments were conducted with typical neutron fluences of $10^{9} \pm 1$ s^{-1} into 4π steradians.

4. RESULTS AND ANALYSIS OF D-T GENERATOR EXPERIMENTS

4.1 Efficiency and Background Measurements

The absolute β^- detection efficiency of the plastic scintillator decay chamber was determined in an experiment with ^{16}N activity. The 7.1 s ^{16}N was produced and transported using the same apparatus, via the $^{16}O(n,p)$ reaction and using ordinary O_2 gas as both target and carrier. The viability of this source had been determined in a previous experiment (Ref. 3). ^{16}N decays with a 69% branch via a 4-MeV end-point β^- followed by a prompt 6.13 MeV γ-ray. This γ-ray was detected with a 5"×5" NaI detector in singles and in coincidence with the β^- particles in the scintillator chamber. The ratio of coincidences to γ-ray singles gives the absolute β^- efficiency for the scintillator chamber. The discriminator thresholds for the PMT signals were adjusted to obtain the optimum efficiency versus noise rate in the chamber. An operating plateau in discriminator settings was observed with the resulting scintillator detector absolute β^- efficiency, $\varepsilon_{det} = 77\%$.

The detector chamber was surrounded by lead bricks to reduce the background counting rate by a factor of about 3. The background count rate was observed to be about 9 s^{-1}. There was no significant change in the background count rate when the DT generator was switched on in the absence of any carrier gas flow.

4.2 Time-Resolved Data.

The characteristic 0.84 s half-lifeof ^{8}Li was observed by taking time-resolved data over many cycles in the Multi-Channel Scaling (MCS) mode of the Canberra 35 analyzer. The data for a run with a 50 ft capillary line and a polyethylene-^{11}B target is shown in figure 2. In this run, the data was scaled in 0.1 s time bins. The transport gas was allowed to flow through the decay chamber for the first 5 seconds of the cycle. This caused the build-up of activity seen in the data. The overflow in channel 50 (i.e. 5 s after the start of the cycle) is noise in the PMT's induced by the vibration of the solenoid valves acting at this point.

This is an inadvertent marker confirming that the inlet-outlet valves were closed at this point (and the bypass valve opened) allowing the decay curve of the activity to be observed. The decay curve was followed for 23 s, and the cycle was repeated. The neutron source was on and the gas flow was maintained through the bypass valve during the decay curve acquisition.

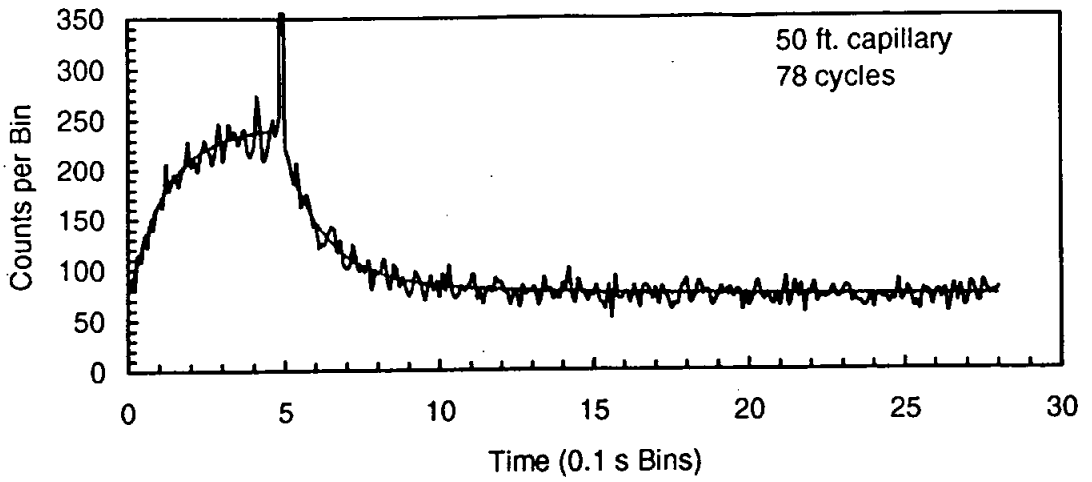

Figure 2. Time-resoved data and fit for a run with a 50 ft. capillary line.

The decay curve in the data in figure 2 clearly shows the presence of a short-lived (≤ 1 s) activity and a constant background. The decay components were further analysed by doing least-squares fits to the build-up and decay portions. The multi-parameter fits were done using the SOLVER function in the Microsoft EXCEL software package.

For the data in figure 2, the build-up curve was fitted with the functional form:

$$y(t) = a_1 + a_2 \times 2^{-\left(\frac{t}{t_{1/2}}\right)} \tag{9}$$

The best fit was obtained with a_1 = ????, a_2 = ???? and $t_{1/2}$ = ???? s. The corresponding mean build-up rate, (log $2/t_{1/2}$), is consistent with the sum of ^{8}Li decay rate (log 2/0.84 s) and the inverse of the mean gas residence time in the chamber.

The decay curve was fitted with a constant plus one or two exponential decay components, i.e. with the function:

$$y(t) = c + a_1 \cdot 2^{-\left(\frac{t-t_0}{t_1}\right)} + a_2 \cdot 2^{-\left(\frac{t-t_0}{t_2}\right)} \tag{10}$$

where the starting time, t_0 was taken to be 5.0 s (or time bin number 50). The parameters a1 and a2 are the number of counts due to each component in the first decay bin (i.e. at

time 5.1 s), while the parameter c is the fitted number of time-independent or background counts per bin. The results of various fits with different combinations of fixed and free parameters are shown in Table 2. The portion of the decay curve which is fitted contains 230 data points (i.e. 23 s)

Table 2: Results of fits to fig. 1 data with different parameters kept free.

Parameters	a_1	t_1 Half-life(s)	a_2	t_2 Half-life(s)	c	χ^2
a_1, c free	162.75	0.84	0	0	75.94	227.7
a_1, t_1, c free	137.5	1.14	0	0	74.6	206.6
a_1,t_1,a_2,c free	137.43	0.97	13.91	13.8	67.8	200.9
All Free	122.01	0.785	29.43	2.95	73.0	199.2
a_1, a_2, c free	143.81	0.84	19.17	13.8	65.5	203.2
a_1, a_2, t_2, c free	126.12	0.84	23.42	3.41	72.82	199.3

Since χ^2/D.O.F.≈ 1 for all the fits, they are all in the right ball-park. For a one component fit (first two rows of Table 2),the data favours a slightly longer half-life than that of ^{8}Li. With two components in the fit (last three rows of Table 2), the χ^2 improves significantly in all cases. In these fits, the shorter component is consistent with the ^{8}Li half-life, confirming that this isotope is observed. While the data favours a ~ 3 s half-life for the second decay component, the fit with this component fixed at the ^{11}Be half-life of 13.8 s (row 4) is only marginally worse. When the amplitudes are extracted with the correlations accounted for, the best fit results obtained for fixed half-lives of 0.84 s and 13.8 s are a_1 = 143.81±10, a_2 = 19.17±3 and c = 65.5±4.

Since these are the fitted number of counts due to each decay component in the first 0.1 s time bin, they have to be divided by (1 - exp(-0.1/$t_{1/2}$)) for each component and further by 78 cycles to obtain the equilibrium fitted count rate per second. Then they have to be divided by the β^- counting efficiency of 0.77 to obtain the equilibrium decay rate, R_{dec}, of each isotope in the decay chamber. To obtain the production rate in the target, the experimental conditions have to be put into equations (2) to (8) to obtain the efficiency factors. For this run, P_{tgt} = 1.4 atm., P_{dec} = 1.0 atm., and Q = 130.4 atm-cc s^{-1}. With V_{tgt} = 60 cc and V_{dec} = 70 cc, we obtain τ_{tgt} = 0.65 s, τ_{dec} = 1.3 s and t_{trans} = 0.668 s. Finally, the total efficiency factors, i.e. the product of the three factors defined in eqn.(3), (6) and (7) for the two isotopes are calculated to be $\varepsilon_{tot}(^8Li)$ = 19.45%, and $\varepsilon_{tot}(^{11}Be)$ = 5.76%. The difference in the efficiencies is mainly due to the short decay chamber turnover time which discriminates against the relatively longer-lived ^{11}Be.

The production rate of the two isotopes is therefore determined to be 92.7 s^{-1} for ^{8}Li and 42.9 s^{-1} for ^{11}Be. The target covered 21.1% of 4π steradians, and the average neutron fluence on it was measured to be 3.8×10^{8} s^{-1}. Thus the measured yields per neutron in this run were:

$$Y_n(^{8}Li) = (3.17 \pm 0.22) \times 10^{-7} \text{ and } Y_n(^{11}Be) = (1.47 \pm 0.17) \times 10^{-7} \quad (11)$$

where the quoted errors are statistical only. The constant term in the fit yields a background rate of 8.4 ± 0.5 s^{-1}.

A time resolved run with 150 ft of transport capillary is shown in figure 3. An analysis similar to the one above gives fitted values of $a_1 = 25.7\pm3$ for a fixed 0.84 s decay component, $a_2 = 11.23\pm3$ for a fixed 13.8 s second decay component, and $c = 42.24\pm3$ for the constant background term. After correction for the bin width of 0.1 s, the β^- detection effiiciency of 0.77, and the 49 time cycles for this data set, the observed decay rates in equilibrium were calculated to be 7.1 s^{-1} for ^{8}Li and 2.99 s^{-1} for ^{11}Be.

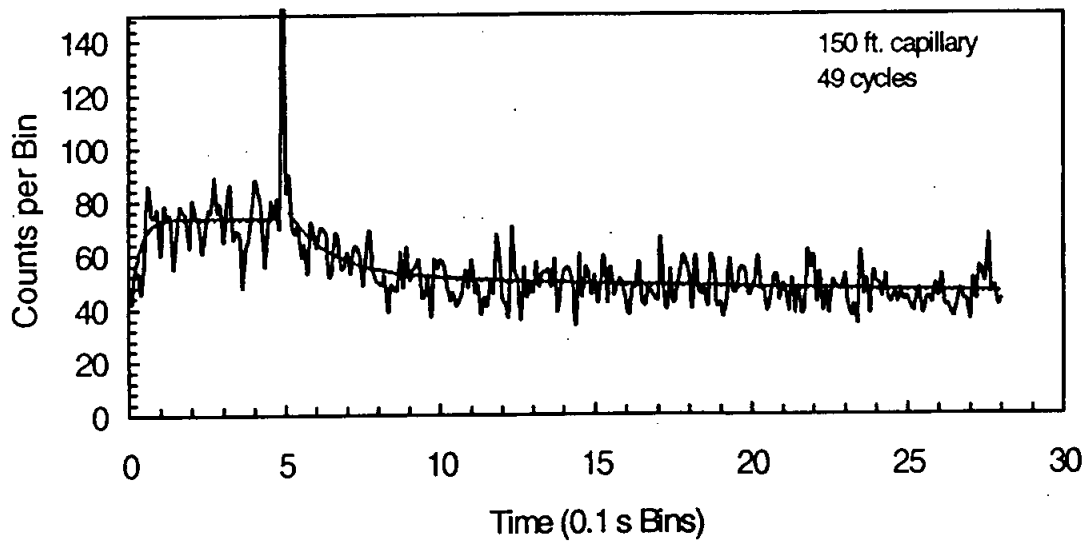

Figure 3: Time-resoved data and fit for a run with a 150 ft. capillary line.

The gas flow conditions for this run were $P_{tgt} = 2.2$ atm, $P_{dec} = 1.0$ atm., and Q = 157.4 atm-cc s^{-1}. Corresponding residence and capillary transport times were therefore $\tau_{tgt} = 0.736$ s, $\tau_{dec} = 1.303$ s and $t_{trans} = 2.68$ s. Total transport efficiencies calculated by multiplying the results from equations (3), (6) and (7) turn out to be ε_{tot} (^{8}Li) = 3.07% and ε_{tot}(^{11}Be) = 3.91%. The overall efficiency for ^{8}Li for this run was much lower than the 50 ft. capillary run because of the increase in the capillary transport time. Finally, the neutron

irradiation rate of the target was measured to be 5.33×10^{8} s^{-1}. The final yields were thus calculated to be:

$$Y_n(^{8}Li) = (4.34\pm0.52) \times 10^{-7}\, n^{-1} \text{ and } Y_n(^{11}Be) = (1.1\pm0.28) \times 10^{-7}\, n^{-1} \qquad (??)$$

The constant term in the fir yields a background count rate of 8.6 ± 0.6 s^{-1}.

4.4 Other Results.

Experiments with the aerosol generator turned off yielded no counts above background. This demonstrated the need for an aerosol carrier for transporting the non-volatile ^{8}Li and ^{11}Be species in contrast to ^{16}N where the target and carrier gas was pure oxygen.

Time resolved runs were also carried out with the previosly mentioned set-up where the decay chamber was a thin-walled aluminum vessel and the β^- particles were detected in a plastic paddle. ^{8}Li yields for the polyethylene-^{11}B target were in good agreement with the later scintillator decay chamber runs. The signal to noise (i.e. efficiency vs. background) levels and neutron fluxes in these earlier experiments were not good enough to unambiguosly resolve the ^{11}Be decay signature. BN targets were also tried in these experiments. The yields from BN were approximately a factor of 2 lower than from the pure ^{11}B-polyethylene targets.

A series of time resolved data were taken with thin polypropylene (PP) cover foils on the polyethylene-^{11}B targets. The purpose was to study the differential attenuation of the ^{11}Be recoil production in order to make a pure ^{8}Li source. The scintillator decay chamber and 50 ft capillary were used for these data. The ^{8}Li yield decreased with increasing polypropylene thickness as expected. However, the weak ^{11}Be signal, and the ambiguity in fitting it precluded any quantitative conclusion about its yield as the dead layer thickness was increased.

Several short runs, without time cycling, and with different pressures and flow conditions were tried. The purpose was to see if the count rate in the detector scaled with the different efficiencies as calculated from equations (3), (6) and (7) The signal in these cases were taken to be the increase in detector counting rates above the previously determined background counting rates. Despite the large uncertainities associated with such rough data, the yield comparisons for all three sets of capillary lengths (50, 100 and 150 ft) were good.

In off-line tests, the decay chamber was counted off-line with a shielded Ge detector after a few days of experimentation. No peaks other than those from natural room background were observed, demonstrating that gross quantities of long-lived activities were not plated out in the chamber. No attempt was made to quantify the level of cleanliness.

An off-line test of the proposed tagging scheme was conducted with a 2" ID, 3" length, flow through gas counter with a 0.0005" central wire. The counting gas was aerosol loaded Helium. α-particles from a 80 Bq ^{241}Am source were detected. Excellent

discrimination for 5.5 MeV α-particles was achieved with a few hundred volts on the wire. The chamber did not appear to suffer any adverse effects from the presence of the aerosol, or from aerosol plate-out even after several hours of running.

5. DISCUSSION AND CONCLUSIONS

The experimental yields of ^{8}Li (Section 4.2) agree within a factor of 2 with the expectations (Section 2.1). An aerosol capture yield of 50% is in fact commonly observed by other groups who use such gas jet systems for studies of short-lived nuclei. The yields for ^{11}Be appear to be consistent with a cross-section which is close to the high end of the range shown in Table 1. However, the yields determined in section 4.2 are subject to the following caveats:

(1) The efficiencies formulated in Section 2.2 assume complete gas mixing in the target and decay chambers. This assumption will in general will cause a larger value of the mean residence time, hence will reduce the target chamber efficiency and increase the decay chamber efficiency from the unmixed case. Regardless of flow conditions however, the assumption of complete mixing is adequate in the case of the target chamber because the wide range of recoil ion energies and resulting ranges in the He gas should cause uniform distribution of these ions in the chamber. In the decay chamber however, small changes in the assumed residence time can potentially have a major impact on the calculated value of ε_{dec} for either one of the radioactive species considered.

(2) Since the recoil ions from the target thermalize in the target chamber by ranging out in the He gas, the ranges of these ions in comparison to the target chamber dimensions becomes an important considerations. These ranges are 7 cm and 4.4 cm for 5.5-MeV ^{8}Li ions at He gas pressures of 1.4 atm. and 2.2 atm. respectively. ^{11}Be ions being heavier and less energetic have a shorter range. Ions which do not range out will hit the walls of the target chamber and will not be transported. Thus the calculated yields would increase with shorter recoil ranges (in He) i.e. for ^{11}Be relative to ^{8}Li and with increasing gas pressure.

(3) The yields calculated here take no account of the possible inefficiency of aerosol particles to capture recoil activities, nor do they account for the plating out of these aerosols due to settling or turbulence on the walls of either of the chambers or in the transport line. Plating out would effectively increase residence times, thus lead to less efficiency for the target chamber and the capillary transport, and increased efficiency for the decay chamber. Another possible effect is that the efficiency of the β^- detector may change with time during the decay curve, due to the change in the geometry of the activity distribution. This effect may be the cause of the difficulty in matching the ^{11}Be half-life in the fits of section 4.2.

Due to these caveats, the yields measured in these experiments should be regarded as lower limits to the actual recoil yield from an ^{11}B target. The yields of ^{11}Be from these experiments are subject to large systematic uncertainities. This yield has been measured in an experiment at the TASCC facility where the NaCl aerosol was collected on a tape

transport system and subsequently counted. Aerosol settling effects and short residence time were thus not a problem.

These experiments demonstrate that there is no loss in capillary efficiency in going from 50 ft to 150 ft of transport line. This bodes well for the SNO calibration scheme where 70 m total transport distance is envisaged. The constant count rate fitted in the decay curve measurements is in excellent agreement with room background measurements, showing that there are no other significant radio-activities produced in this scheme.

For the purpose of doing calculations for the proposed calibration scheme for SNO, we adopt a yield of 3×10^{-7} ^{8}Li atoms per 14-MeV neutron incident on a ^{11}B-polyethylene(10%) target foil. The yield for ^{11}Be has been adopted as 2×10^{-8} n^{-1} (from the TASCC experiment). It is proposed to install a small commercially obtained DT generator producing a maximum of 10^{8} n s^{-1} in the underground SNO laboratory. Calculations and optimizations carried out as outlined in section 2 show that it should be possible to obtain a ^{8}Li decay rate of 1 s^{-1} in a decay chamber inside the SNO D_2O volume.

ACKNOWLEDGEMENTS

We would like to acknowledge Emmanuel Bonvin for pointing out to us the efficacy of ^{8}Li as a calibration source for SNO, and the possibility of tagging its decays in a wire chamber. Hamish Leslie suggested the ^{11}B(n,α) reaction. Bill Frati did the Monte-Carlo yield calculation. Vern Koslowsky and Erik Hagberg provided much technical know-how and moral support. Amar Arneja provided excellent support in operating the DT generator.

References

1. Table of radioactive Isotopes. Edgardo Brown and Richard B. Firestone, edited by Virginia Shirley, (John Wiley and Sons, 1986).

2. V. McLane, C. L. Dunford and P. F. Rose, Neutron Cross Sections Vol 2. (Academic Press 1988)

3. B. Sur, E. D. Earle, E. Gaudette and R. Deal, ^{16}N: A Calibration Source for SNO, SNO-STR-93-041.